AD-A148 756 THE GROWTH OF LARGE DIAMETER SINGLE CRYSTALS BY VERTICAL SOLIDIFICATION OF THE MELT(U) ARMY MATERIALS AND MECHANICS RESEARCH CENTER WATERTOWN MA 1/1

UNCLASSIFIED J L CASLAVSKY AUG 84 AMMRC-TR-84-34 F/G 20/2 NL

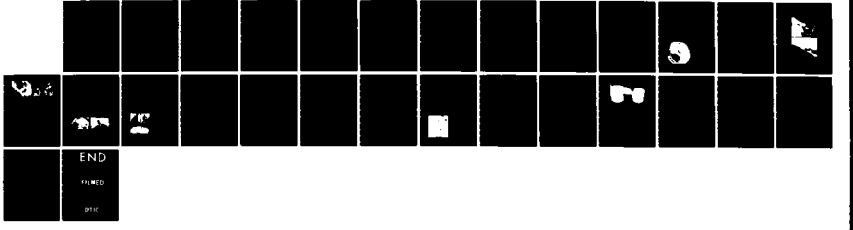

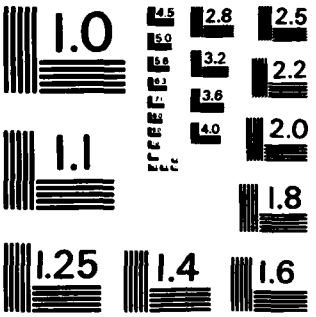

MICROCOPY RESOLUTION TEST CHART
NATIONAL BUREAU OF STANDARDS-1963-A

AMMRC TR 84-34

AD

THE GROWTH OF LARGE DIAMETER SINGLE CRYSTALS BY VERTICAL SOLIDIFICATION OF THE MELT

JAROSLAV L. CASLAVSKY
CERAMICS RESEARCH DIVISION

August 1984

Approved for public release; distribution unlimited.

ARMY MATERIALS AND MECHANICS RESEARCH CENTER
Watertown, Massachusetts 02172

The findings in this report are not to be construed as an official Department of the Army position, unless so designated by other authorized documents.

Mention of any trade names or manufacturers in this report shall not be construed as advertising nor as an official indorsement or approval of such products or companies by the United States Government.

DISPOSITION INSTRUCTIONS

Destroy this report when it is no longer needed
Do not return it to the originator

UNCLASSIFIED

SECURITY CLASSIFICATION OF THIS PAGE (When Data Entered)

REPORT DOCUMENTATION PAGE		READ INSTRUCTIONS BEFORE COMPLETING FORM
1. REPORT NUMBER AMMRC TR 84-34	2 GOVT ACCESSION NO.	3. RECIPIENT'S CATALOG NUMBER
4. TITLE (and Subtitle) THE GROWTH OF LARGE DIAMETER SINGLE CRYSTALS BY VERTICAL SOLIDIFICATION OF THE MELT		5 TYPE OF REPORT & PERIOD COVERED Final Report 6 PERFORMING ORG. REPORT NUMBER
7. AUTHOR(s) Jaroslav L. Caslavsky		8. CONTRACT OR GRANT NUMBER(s)
9. PERFORMING ORGANIZATION NAME AND ADDRESS Army Materials and Mechanics Research Center Watertown, Massachusetts 02172 AMXMR-MC		10 PROGRAM ELEMENT, PROJECT, TASK AREA & WORK UNIT NUMBERS D/A Project: 1L1621054AH42
11. CONTROLLING OFFICE NAME AND ADDRESS U.S. Army Materiel Command Alexandria, Virginia 22333		12. REPORT DATE August 1984 13. NUMBER OF PAGES 22
14. MONITORING AGENCY NAME & ADDRESS(if different from Controlling Office)		15. SECURITY CLASS (of this report) Unclassified 15a. DECLASSIFICATION/DOWNGRADING SCHEDULE

16. DISTRIBUTION STATEMENT (of this Report)

Approved for public release; distribution unlimited.

17. DISTRIBUTION STATEMENT (of the abstract entered in Block 20, if different from Report)

18. SUPPLEMENTARY NOTES

Presented at the Fifth International Summer School on Crystal Growth and Material Research, Davos, Switzerland

19 KEY WORDS (Continue on reverse side if necessary and identify by block number)

Crystal growth
Crystals
Solidification

20 ABSTRACT (Continue on reverse side if necessary and identify by block number)

(SEE REVERSE SIDE)

DD FORM 1 JAN 73 1473 EDITION OF 1 NOV 65 IS OBSOLETE

UNCLASSIFIED

SECURITY CLASSIFICATION OF THIS PAGE (When Data Entered)

Block No. 20

ABSTRACT

Growth of large diameter single crystals, especially of phases which melt at high temperatures and have a high specific gravity, is governed by conditions that quite differ from those which occur during the growth of crystals whose diameter does not exceed 50 mm. This paper defines and analyzes these special conditions and delineates their effect on crystal growth. It is also shown that in spite of the presence of negative factors which are inherent to the growth process of large diameter single crystals, these adverse factors, if recognized properly, can be brought under control to such a degree that the growth of large diameter single crystals can be achieved. The vertical solidification of melt method (VSOM) is described. This method produces large single crystals, even for binary mixtures with a steep liquidus. Neodymium-doped yttrium aluminum garnet (Nd:YAG) crystals have been grown 75 mm in diameter and 100 mm high. These crystals are also water clear. Both size and perfect crystallinity are important for application to lasers.

CONTENTS

	Page
INTRODUCTION.	1
STATEMENT OF THE PROBLEM.	1
Crack Formation in Large Diameter Single Crystals.	5
Second Phase Segregation	9
CONTROL OF THE FACTORS AFFECTING THE GROWTH OF LARGE DIAMETER SINGLE CRYSTALS.	11
CONCLUSIONS	19

INTRODUCTION

In 1918, Czochralski[1] developed a method for measuring speed of crystallization of metals. This technique soon found its general use in crystal growth, at first in the formation of wire-like single crystals and later in the production of a great majority of single crystals grown from the melt. However, there are some limiting factors in Czochralski's technique, which prevent its application to the growth of large diameter single crystals, particularly from materials which simultaneously have a high melting point and high specific gravity, and are also multi-component systems.

In 1924, Ströber[2] introduced a technique which was based on cooling a melt confined in a hemispherical dish by resting it on a water-cooled heat sink. This process is most suitable for the growth of single crystals which possess a unique crystallographic axis along which much greater heat conductivity is associated than in other directions. The disadvantage of this technique is that the loss of a thermal gradient towards the end of solidification causes an uncontrollable growth, resulting in low quality crystals.

In 1974, Viechnicki and Schmid[3] overcame the disadvantages of the latter method by controlling both the nucleation and loss of the thermal gradient, thus enabling growth of large single crystals. However, this Heat Exchanger Method (HEM) proves to be useful for growing large diameter single crystals mainly from single component systems.

Recently, in our laboratory a method was developed for growing laser quality single crystals from materials belonging to binary or even to more complicated systems. This technique is called the Vertical Solidification of the Melt (VSOM), because the solidification commences at the bottom of the crucible containing the melt. Advantages as well as problems associated with the VSOM technique will be analyzed in this paper.

STATEMENT OF THE PROBLEM

Production of single crystals from the melt involves an arrangement of conditions in which atoms of the melt "freeze out" on a nucleus or seed crystal and perpetuate the lattice array of the nucleus.

1. CZOCHRALSKI, J. Zeits. Physics. & Chem., v. 8, 1918, p. 219.
2. STRÖBER, F. Zeits. f. Kryst., v. 61, 1925, p. 299.
3. STRONG, J. Phys. Rev., v. 36, 1930, p. 1663.

If the crystal is to be grown at the expense of the liquid, whose temperature is at all points above the melting point, then the latent heat can only be removed by conduction down through the already formed crystal. Thus, a temperature gradient must be maintained along the length of the crystallized solid.

In the majority of the crystal growth techniques, the propagation of the solid-liquid interface is achieved by drawing the crystal through a thermal gradient or by moving the furnace itself. This motion causes vibrations, and thermal fluctuations which may deleteriously affect the growth of crystals, especially large diameter crystals destined for laser purposes.

As previously mentioned, the Czochralski method is not well suited for the growth of large diameter, laser quality single crystals from materials of high specific gravity and high melting temperature. These two factors combined, especially in the presence of vibrations caused by pullers, increase the probability of stress occurrence in the neck of the crystal. Generally such stress is a leading source of crack nucleation. Furthermore, thermal fluctuations during the growth can cause defects to form in large diameter single crystals.

The Ströber technique eliminates the problem of vibrations by simply moving the thermal field through the system instead by moving the crucible or the furnace. Its mode of cooling is designed in such a way that the soldification commences at the bottom of the container and proceeds upwards. The upward thermal gradient has a stabilizing effect on the growth, but in order to eliminate the polycrystalline growth, the nucleation must start from a single nucleus, i.e., from almost a point. In 1930, using the Ströber technique, Strong[4] grew 100 X 100 mm alkali halides crystals; however, at the end of the process, he lost growth control due to an insufficient thermal gradient which caused the upper portion of the crystal to be cloudy.

Viechnicki and Schmid[3] overcame both the nucleation problem and loss of the thermal gradient by placing the seed crystal above a helium-cooled heat exchanger. Cylindrical sapphire single crystals were grown, 130 mm high, 250 mm in diameter, with a low density of dislocations and almost

4. VIECHNICKI, D., and SCHMID, F. *Crystal Growth Using the Heat Exchanger Method (HEM).* J. Crystal Growth, v. 26, 1974, p. 162.

free of grain boundaries.[5] The Heat Exchanger Method (HEM), however, did not prove to be suitable for the growth of large diameter laser quality single crystals of compositions which belong to binary systems, with a steep liquidus. The reason for this unsuitability seems to be associated with principles which, unfortunately, are inherent in the technique. In the HEM, the melt is kept at constant temperature while growth of the crystal is controlled by the thermal gradient within the solid, and directed by the helium flow in the heat exchanger. Since the temperature of the solid-liquid interface is constant at any given point, the melt temperature is not influenced for all practical purposes either; therefore, it remains uniform in almost the entire volume of the melt. In order to sustain the growth, the thermal gradient in the solid has to be continuously increased. At the beginning of the process, the melt has a comparatively large volume while the crystal growth has to originate from a relatively small seed crystal. In a homogeneous medium, heat propagates in a straight path. Therefore, the solid-liquid interface at the beginning of the solidification takes a hemispherical shape, and consequently the growth becomes three dimensional. The difference in shapes of the hemispherical interface and of the melt, which is contained in a cylindrical crucible, causes the growth rate to vary in the melt due to differences ($\Delta T/\ell$) in all directions perpendicular to the tangents drawn at any given point of the interface. (For the definition of $\Delta T/\ell$, see Figure 1.) Hence, as the growth progresses, curvature of the solid-liquid interface becomes more and more convex, i.e., takes on a paraboloid-like shape which leads to a formation of bizarre pear-shaped interfaces in the last stages of the solidification process (Figure 2).

NOTE: The liquidus of two different congruently melting compounds, in the close proximity of the compounds' melting point, may have an entirely different character. Figures 3a and 3b depict two rather extreme types of liquidus curves. Compounds with a melting behavior described by the type of liquidus shown in Figure 3a, and naturally those of single component systems, are easily grown as single crystals, since only minor temperature adjustments are required during the growth, even if significant composition changes occur in the melt. On the other hand, growth of single crystals

from a melt with compositions characterized by a liquidus shown in Figure 3b, is strongly dependent on the equilibrium temperature. Hence, even small deviations of the melt composition would require major readjustments of the growth temperature.

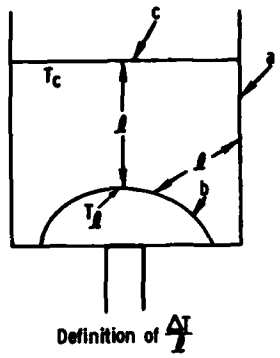

Figure 1. Shows melt confined in cylindrical crucible a; convex solid-liquid interface b; and melt surface c. T_i is a temperature of solid-liquid interface T_c is the temperature at the surface of the melt and ℓ is a perpendicular drawn to tangent at any point of solid liquid interface, hence $(T_c - T_i/\ell) = (\Delta T/\ell)$.

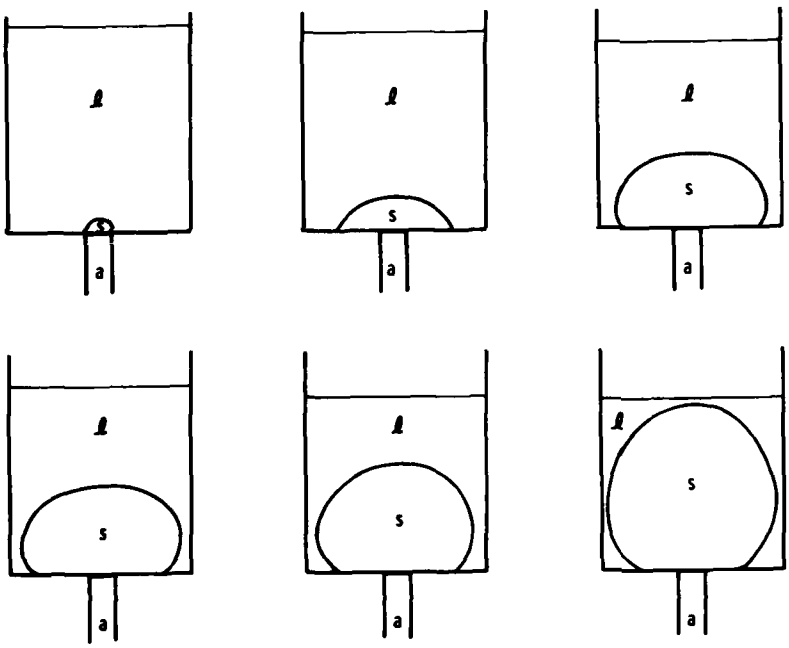

Figure 2. Change of the shape of the solid-liquid interface with progressing growth in HEM technique; ℓ = melt, s = solid, and a = helium heat exchanger.

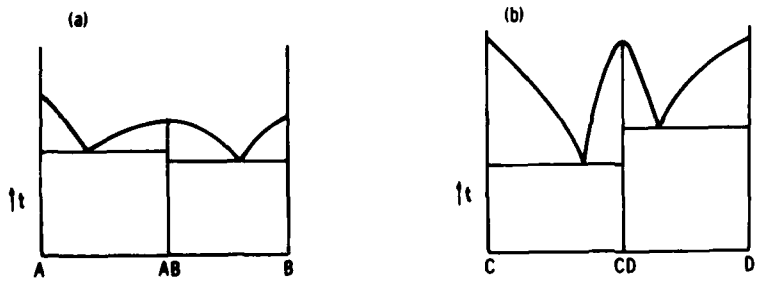

Figure 3. Liquidus curves depicting extremes in melting differences of two hypothetical binary compounds.

Crack Formation in Large Diameter Single Crystals

Until now the discussion of problems associated with the growth of large diameter single crystals was focused on employing the well-established growth techniques and adapting them for a scale-up of crystal diameter. Yet, the problems may also have other origins which may or may not be solely inherent in the techniques of growth. They may be traced, rather, to the specific conditions and mechanisms of the growth of large diameter crystals, or to origins which even have not been sufficiently identified. In spite of that, if the problem is correctly recognized and conditions of the growth amended, large diameter crystals may be grown successfully, as is documented in the case of growth of large sapphire single crystals.

Thermal oscillations generally affect the quality of crystals of any size. If we take a system in which the solid-liquid interface has a convex shape to the melt, then, due to the anistropy of the growth directions, the interface will take on a faceted shape, as seen in Figure 4. These facets form pockets capable of trapping inclusions which can be permanently imbedded in the crystal. An interface of an incongruent particle in the crystal matrix can accept or emit point defects. At a given temperature, the crystal matrix contains an equilibrium concentration of point defects.

Figure 4. Optical photograph of decanted interface of 200 μm diameter sapphire crystal showing pockets formed by facets. The $(10\bar{1}2)$ plane is in the plane of the photograph.

On changing the temperature, this concentration will arrive at a new equilibrium value by drawing point defects from or depositing them into the interface between the matrix and the particle. This results in a change in volume of the hole containing the inclusion, leaving the size of the particle itself unchanged. The misfit thereby created, can develop stresses large enough to nucleate prismatic loops around the particle. If during the crystal growth temperature cycles, a procession or processions of prismatic loops develops in the crystal matrix (see Figure 5a), the accompanying stress to each of the individual loops of the procession is added consonantly. If the resolved value of the emanating stress from the procession of the loops exceeds binding forces of a weak crystallographic plane, then a crack may nucleate in the growing crystal (Figure 5b). This type of crack formation is of a general nature and can be found regardless of the size of the crystal diameter.

Another factor which may lead to crack formation is concentration of stresses in the area of the crystal's neck by the crystal's weight. This stress may occur under conditions which are typical for the Czochralski method, namely, when large diameter single crystals of a high specific gravity are grown. The critical period occurs after the seed is dipped into the melt and the neck of the crystal is formed. To assure the single crystallinity of the growth, the neck diameter has to be increased very rapidly to the final diameter of the crystal. With increasing diameter, the weight of the crystal increases with r^2, so that at some point the crystal's weight will set stress in the neck of the crystal. This stress activates the dislocation sources in the growing crystal. In the case of a large diameter single crystal, numerous dislocation sources are activated simultaneously, causing formation of dislocation tangles[5] (Figure 6). Under stress, the edge dislocation will glide (see Figure 7), but in specific directions only. Due to this glide, edge dislocations form tilt grain boundaries in the crystal,[6] where the magnitude of the tilt of the grain boundary is indirectly proportional to the spacings between the dislocations and, therefore, also to the stress. Hence, magnitude of the tilt of a grain boundary formed by this mechanism is a function of the

5. CASLAVSKY, J. L., GAZZARA, C. P., and MIDDLETON, R. M. *The Study of Basal Dislocations in Sapphire.* Phil. Mag., v. 25, 1972, p. 35.
6. CASLAVSKY, J. L., and GAZZARA, C. P. *Dislocations Behaviour in Sapphire Single Crystals.* Phil. Mag., v. 26, 1972, p. 961.

stress in the neck of the crystal, and thus it depends on the crystal's weight, which is proportional to the specific gravity of the material. In other words, the frequency of the grain boundary formation, as well as

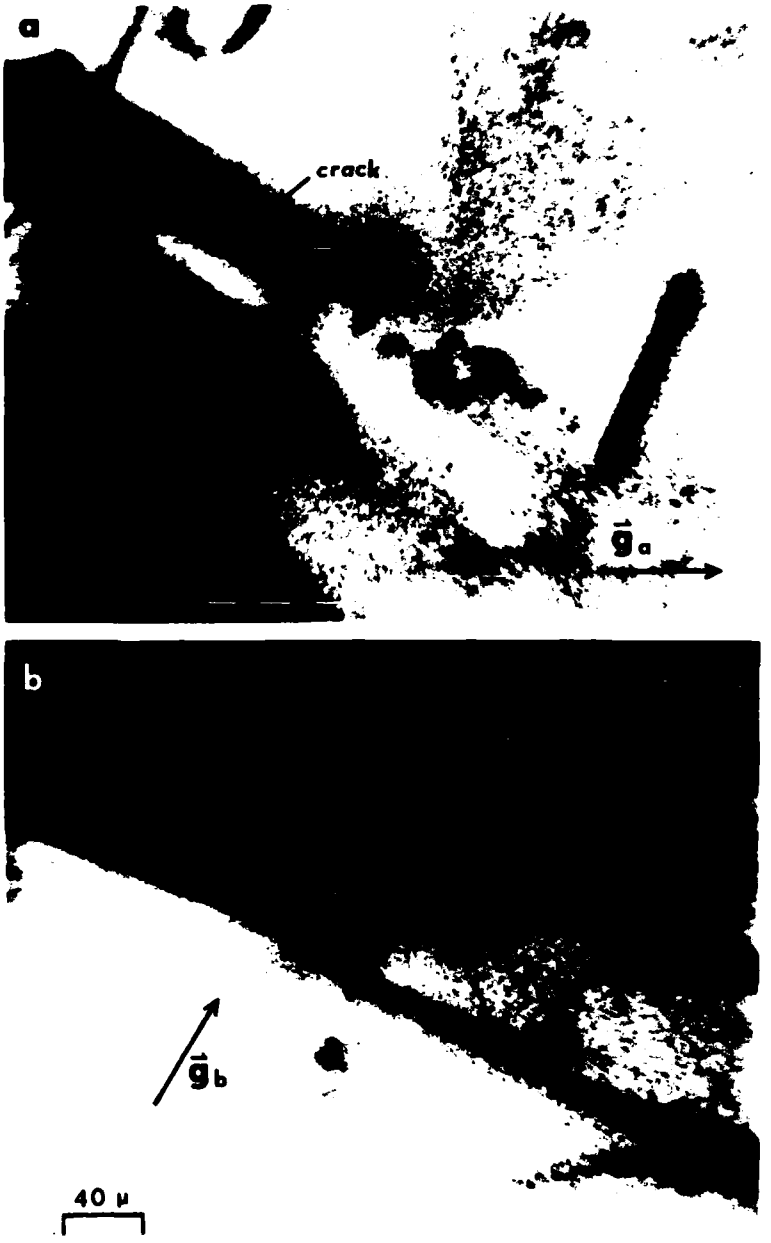

Figure 5. X-ray topographs of two incoherent inclusions [indicated by arrows in plate (b)] in sapphire single crystal. Plate (a) shows two processions of prismatic loops. In plate (b) loops are in extinction; they nucleated crack indicated by arrow in plate (a). Ag K_{α_1} radiation.

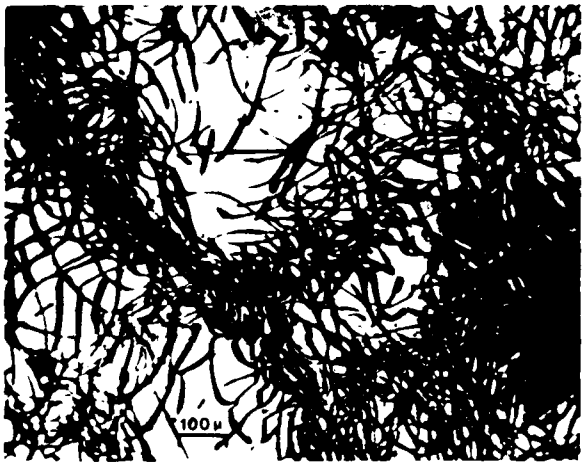

Figure 6. X-ray topograph of dislocation tangles in sapphire single crystal. Note a formation of low-angle grain boundaries. Ag $K\alpha_1$ radiation.

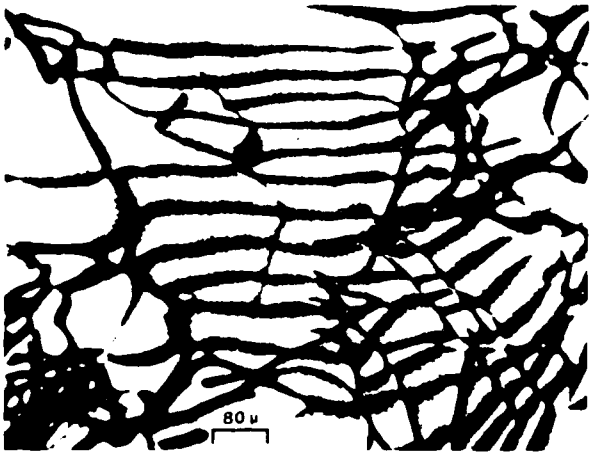

Figure 7. X-ray topograph of edge dislocations gliding under the stress in a sapphire single crystal. Ag $K\alpha_1$ radiation.

the magnitude of the grain boundary angle, is directly proportional to the rate with which the crystal diameter increases from the neck region. Based on experimental data obtained during the growth of large diameter single crystals of refractory oxides, it was found that if the grain boundary is perpendicular to the stress vector, and the tilt angle of the boundary exceeds 7°, then there is a 50% probability that the grain boundary will nucleate a crack during the plastic brittle transformation. The higher the tilt angle, the higher is the probability of crack nucleation. Since the probability of formation of a high angle boundary increases with the increase in the diameter, this mechanism of crack nucleation is likely to occur under the conditions of the Czochralski method, or any other method where the crystal "hangs by its neck." In other words, since the crack nucleation is directly correlated with the crystal's weight, by the Czochralski method, there is a lesser probability of crack formation in growing large diameter silicon single crystals than in growing sapphire crystals of the same size, in spite of the fact that both materials belong to single component systems. Hence, if growth of large diameter single crystals is plagued by the formation of cracks, a detailed study of dislocation confirgurations is recommended in order to find out if the reason is in the choice of the method or in an inadequate temperature control or some other factor.

Second Phase Segregation

Segregation of a second phase generally occurs during the crystal growth due to constitutional supercooling. (In laser crystals, second phase particles are called scattering centers.) This phenomenon can be caused either by impurities or by any material whose composition belongs to a binary system with a steep liquidus. In the former case, the remedy is easily at hand; in the latter case, nucleation of second phase particles is frequently traced to the curvature of the solid-liquid interface. Figures 8 and 9 are photographs of cross sections of sapphire and 1.0 At% Nd:YAG single crystals respectively, both crystals grown by the HEM technique. A highly curved interface is seen in both crystals, but there is an absence of scattering centers in the sapphire crystal, while a high density of second phase particles is deposited in the Nd:YAG crystal. Since both materials have a high melting point, it was possible to grow both types of the crystals under almost identical conditions. The difference in the crystal quality is because sapphire is a single component refractory oxide, while YAG is a binary compound of refractory oxides, whose melting behavior is characterized by a steep liquidus. If such a compound is grown on a curved interface inherent in the HEM technique, variations of $\Delta T/\ell$ in the melt will cause constitutional supercooling and consequently growth instability. Constitutional supercooling is relieved by a compositional change in the liquid resulting in a depostion of second phase particles

Figure 8. Optical photograph of a cross section of sapphire single crystal. Before the completion of solidification the remaining melt was decanted to reveal the shape of solid-liquid interface. Crystal grown by HEM.

Figure 9. Optical photograph of the cross section of a 1 At% Nd:YAG single crystal grown by HEM technique.

along the solid-liquid interface. After the constitutional supercooling is eliminated, the controlled growth is restored. However, the process will repeat itself, leaving alternating clear and translucent bands in the crystal (Figure 9). The geometrical conditions in the HEM apparatus were rearranged to simulate VSOM to enable the Nd:YAG crystals to be grown on a planar interface. The optical photograph in Figure 10 shows a vertical cross section through such a crystal. This photograph shows that the crystal grows from an almost planar interface. There are no layers formed due to the constitutional supercooling. The presence of second phase particles observed in this case and the mechanism of their formation were described by Caslavsky and Viechnicki in 1980.[7]

Planar solid-liquid interface is essential for growing good quality single crystals. But as shown experimentally, it is difficult to maintain it during the entire period of the growth of a large diameter single crystal.

Hence, in order to grow the large diameter, laser quality single crystals form a material which simultaneously comprises all of the properties discussed above, one has to select a growth technique which would enable the following:

a. support of the growing crystal preferably along its entire diameter (rather than having crystal hanging from a narrow seed);

Figure 10. Optical photograph of the cross section of a 1 At% Nd:YAG single crystal grown by VSOM technique.

7. CASLAVSKY, J. L., and VIECHNICKI, D. *Melting Behaviour and Metastability of Yttrium Aluminum Garnet (YAG) and $YAlO_3$ Determined by Optical Differentical Thermal Analysis.* J. Mater. Sci., v. 15, no. 7, 1980, p. 1709.

b. determination of the crystal diameter by the container shape rather than by balancing the heat flow through the system;

c. elimination of mechanical vibrations by application of a mobile thermal field instead of moving the furnace or the crucible or the crystal itself.

Such a crystal growth technique, capable of growing large diameter single crystals from even complicated melts, was developed in our laboratory, and has been named the "Vertical Solidification of the Melt" (VSOM). The method is examined in detail in this paper.

CONTROL OF THE FACTORS AFFECTING THE GROWTH OF LARGE DIAMETER SINGLE CRYSTALS

Previous paragraphs have discussed parameters with a negative influence on the growth of large diameter single crystals. A thorough analysis of these factors revealed that they are intrinsic to the process; hence they can not be eliminated, but their negative effect can be minimized by a combination of compensating conditions. This leads to the creation of a new crystal growth technique which maximizes the potential for growing large diameter single crystals from melts of a wide variety of compositions. However, to ensure smooth operation of the technique, the following conditions must be concurrent and co-operative, and must be observed so that they are under control all the time:

1. The growing crystal must be supported on its entire cross section.
2. Mechanical vibrations must be eliminated.
3. The solid-liquid interface has to become planar on the macroscopic scale, commencing at a specific point, and must remain so until the end of solidification. Accordingly, the Vertical Solidification of the Melt method was developed in our laboratory, VSOM implies the method's main feature, i.e., to respect the nature of the direction of solidification. An apparatus for the crystal growth by vertical solidification was designed and built at the Army Materials and Mechanics Research Center.

At this point, it is proper to discuss separately all the crucial factors which contributed to the design of this apparatus then the analysis and resolution of these factors into the new technique.

The easiest requirement to fulfill was that of supporting the entire cross section of the growing crystal. The material to be solidified was simply placed in a cylindrical container with a diameter of the required crystal size. To commence solidification at a single point and in a

single crystalline mode, a seed crystal was placed in the center of the bottom of the container. The entire charge of the material had to be melted first; hence, in order to protect the seed crystal from melting, the crucible was rested on a cold finger which kept the seed crystal below melting temperature, hence, preventing melting. Then during the period of shaping the solid-liquid interface, and especially during the entire period of the crystal growth, this cold finger takes on the function of a heat sink, thus having a crucial importance for controlling the crystal growth.

Mechanical vibrations were eliminated by the formation of a suitable heat zone which imposes on the solid as well as on the liquid, a thermal field whose isotherms must be parallel with the bottom of the crucible and have an upward gradient. In order to obtain the driving force for the crystal growth, the thermal field is propagated through the system in the desired fashion and rate. This required function is derived from two optical automatic pyrometers (#1 and #2 as illustrated on Figure 11). The basic idea of the design is an follows: pyrometer #1 senses the temperature of the black body and thus controls the desired temperature of the whole system. Pyrometer #2 observes the temperature of the content of the crucible, i.e., it controls the temperature of the melt. In order to start the growth, the temperature of the black body is slightly lowered. Since the heat capacity of the content of the crucible is significantly higher than the black body heat capacity, a temperature difference occurs between the black body and the melt temperature. This difference is seen by optical pyrometers, translated to an appropriate electrical signal and fed into a microprocessor whose program is designed to control the temperature decrease of the black body as a function of ΔT. In this case ΔT is a difference between the temperature of the black body and the surface of the melt. In other words, the rate of temperature decrease of the black body is controlled by the program as a function of the temperature difference between the crucible content and black body. This has a crucial importance. During solidification of crystals with large cross section, a significant amount of a latent heat is developed on the interface; hence, this heat influences the melt temperature. This change is sensed by pyrometer #2, whose signal in turn corrects the signal of pyrometer #1. This type of control enables programing the propagation of the thermal field with

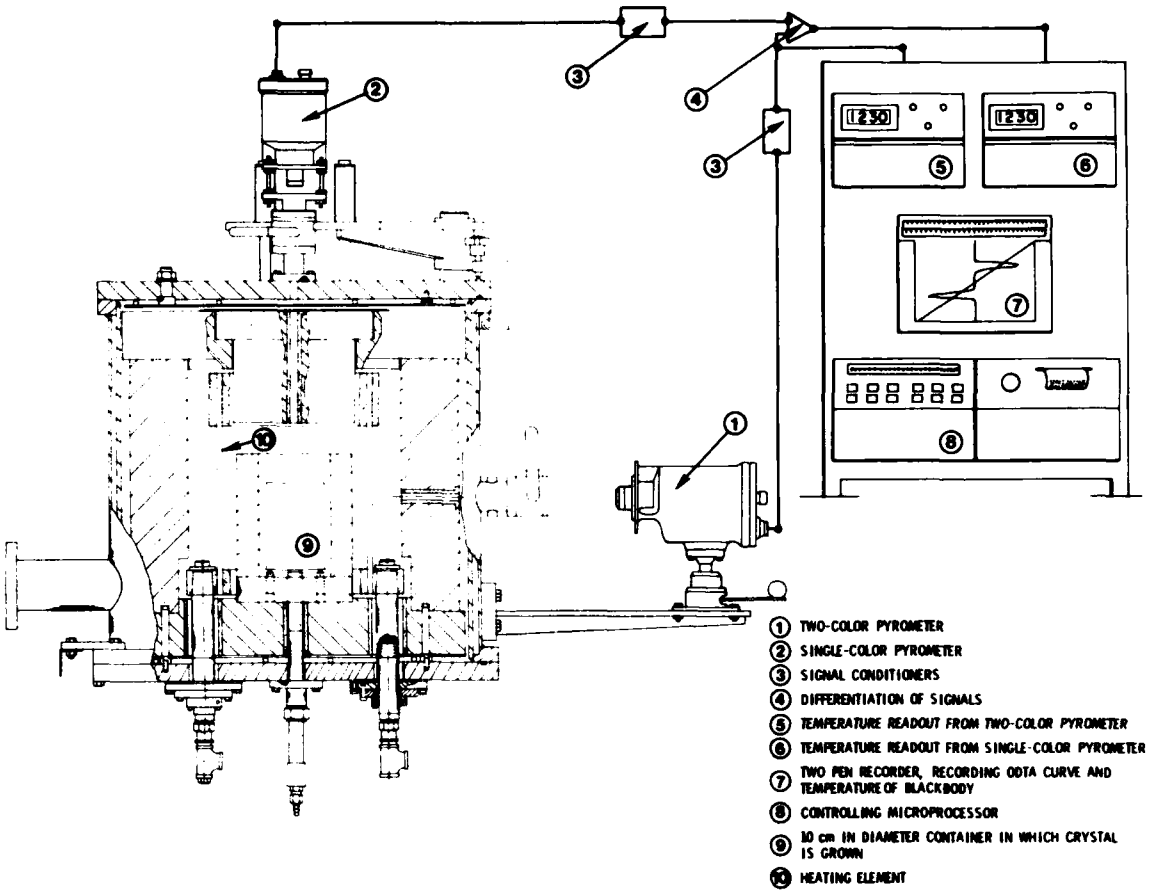

Figure 11. Schematic of crystal growth furnace for vertical solidification of the melt (VSOM).

an accuracy of ±1°C in the temperature range between 1600°C to 2100°C, and the rates of temperature decrease between 2.0 and 0.1°C/h; i.e., the temperature of the thermal field, measured at any point along the vertical axis of the field, can be controlled with an accuracy ±1°C in the given range, and the temperature at such a point of the thermal field can be either decreased or increased as slowly as 0.1°C/h linearly in the given range. In principle, this is the driving force for the crystal growth--a very accurate control. However, to keep isotherms of the upward thermal field mutually parallel, the latent heat of solidification has to be removed from the system down through the already crystallized solid and down into the heat sink. Therefore, in order to grow a single crystal by vertical solidification and in a controlled manner on a flat interface, the heat flow through the heat sink has to be equal to the net heat flow through the interface conducted down through the already crystallized charge. The heat transfer equation describing the heat flow through the interface and the solid may be written as follows:

$$K_S A_s \frac{dT}{dx_s} - K_\ell A_\ell \frac{dT}{dx_\ell} = AL\rho \frac{dx}{dt} \quad (1)$$

where: K = thermal conductivity

A = cross section area of the charge

T = temperature

x = a coordinate measured along the vertical axis of the system

ρ = density of the material

L = latent heat of the crystallizing material (suffixes s, l and h relate to the solid and liquid phase and to the heat sink respectively see graphical illustration in Figure 12).

Since the cross section A_s and A_ℓ and the interface A are approximately equal, we may write that:

$$K_s G_s - K_\ell G_\ell = RL\rho \quad (2)$$

where: G = temperature gradient

R = growth rate.

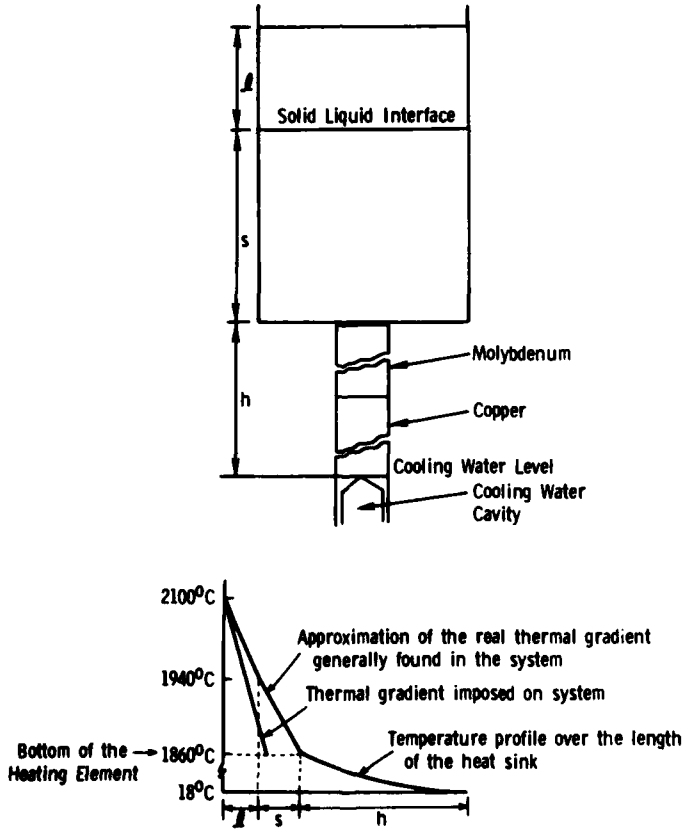

Figure 12. Graphic illustration of cross section of the crucible and the heat sink.

In this case, the growth rate is the movement of the interface and the rate of the growth of the crystal is governed by the rate at which the latent heat is extracted from the system by the heat sink. The heat flow ϕ through the heat sink can be expressed:

$$\phi = K_h A_h \frac{dT}{dx_h} \tag{3}$$

and in the first approximation:

$$RL\rho = K_h A_h \frac{dT}{dx_h}. \tag{4}$$

Because of complicated boundary conditions and the practical impossibility of determining the exact position of the interface, Equation 4 cannot be solved numerically. Therefore, ϕ has to be determined experimentally, from the grown crystal. If the heat sink removes an insufficient amount of heat, i.e., if

$$RL\rho > K_h A_h \frac{dT}{dx_h}, \tag{5}$$

then a dendritic growth is observed (see Figure 13). Or if

$$RL\rho < K_h A_h \frac{dT}{dx_h}, \tag{6}$$

i.e., if the heat sink removes an excessive amount of heat, the interface will become convex (see Figures 8 and 9).

Figure 13. Optical micrograph of decanted interface of sapphire crystal grown by VSOM technique under $RL\rho > K_h A_h (dT/dx_h)$ condition. [0001] directions is in the axis of the sapphire dendrite. The crystal was grown in [5052] direction perpendicular to the plane of photograph.

Once the direction of an error is known, the heat flow capacity of the heat sink can be corrected in the following way. Designing of the heat sink for growing large diameter crystals with a melting point above 1600°C is influenced by two important factors. Total heat flow in the heat sink is considerable; hence, it has to be made from a material with high thermal conductivity. Copper is a material with high heat conductivity, but copper is not practical with high temperatures because its melting point is low (1083°C). Nevertheless, the main body of the heat sink (#2, Figure 14) is designed to be made of copper, but it is extended by tungsten to the region of the high temperature (#1, Figure 14). The dimensions of the surface are determined by diameter "f" (Figure 14) and its optimal value was found experimentally to be 1/15 of the interface surface area. Value of "a" has to be determined by trial and error. To approach closely Equation 4, the fine tuning of the ϕ value can be achieved by adjusting dimensions "c" and "e" (Figure 14), to a degree that the heat flux ϕ required for steady growth can be controlled only by moderating the flow of the cooling water through the heat sink. This is done at 50% of maximum cooling water flow at the water temperature 2°C higher than the water temperature required during the growth.

In our laboratory we have focused on growing large diameter crystals of refractory oxides with the melting point in the 1800° to 2100°C range. For this reason, resistively heated graphite furnaces are used. To protect the graphite and the heat sink including the molybdenum crucible, a low vacuum is used, approximately 5 times 10^{-2}. At first conventional "ribbon" type element was used, but electric current in that type of element (Figure 15 on the right hand side) is prone to develop alternating hot and cold spots which effect circumferential and axial temperature gradient. Such an element, therefore, proved useless for the growth of crystals by the vertical solidification of the melt. In 1976, a graphite element called a "bird cage" was designed and built (Figure 15, left). This element consisted of a complete bottom ring, a split upper ring and forty tapered graphite rods connecting the rings. These rods are tapered proportionally to the required upward thermal gradient. Originally, in the first design of the element, the power feeds were attached to the upper element ring. Because of the heat developed by the element, and also because of the need to operate the

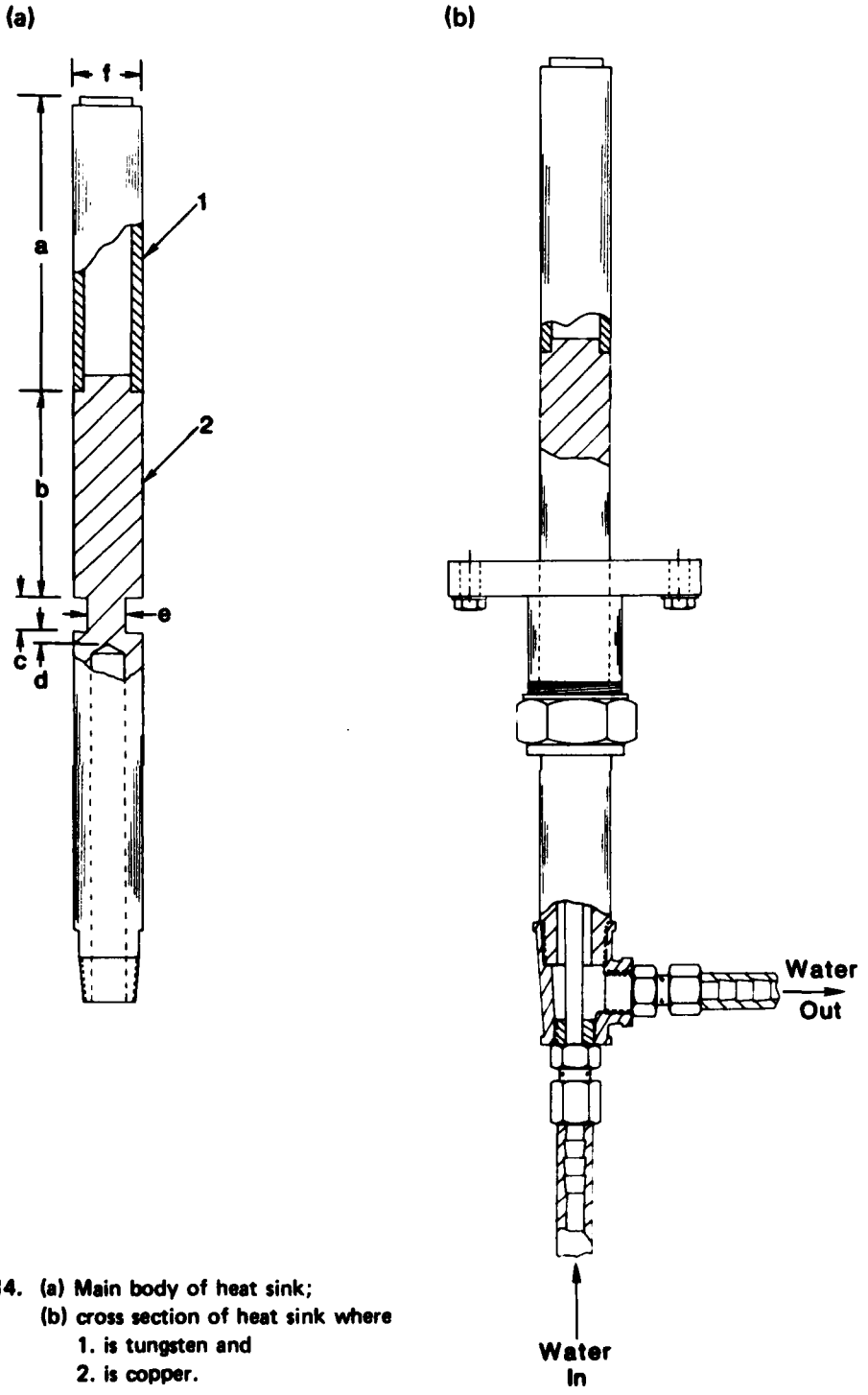

Figure 14. (a) Main body of heat sink;
(b) cross section of heat sink where
1. is tungsten and
2. is copper.

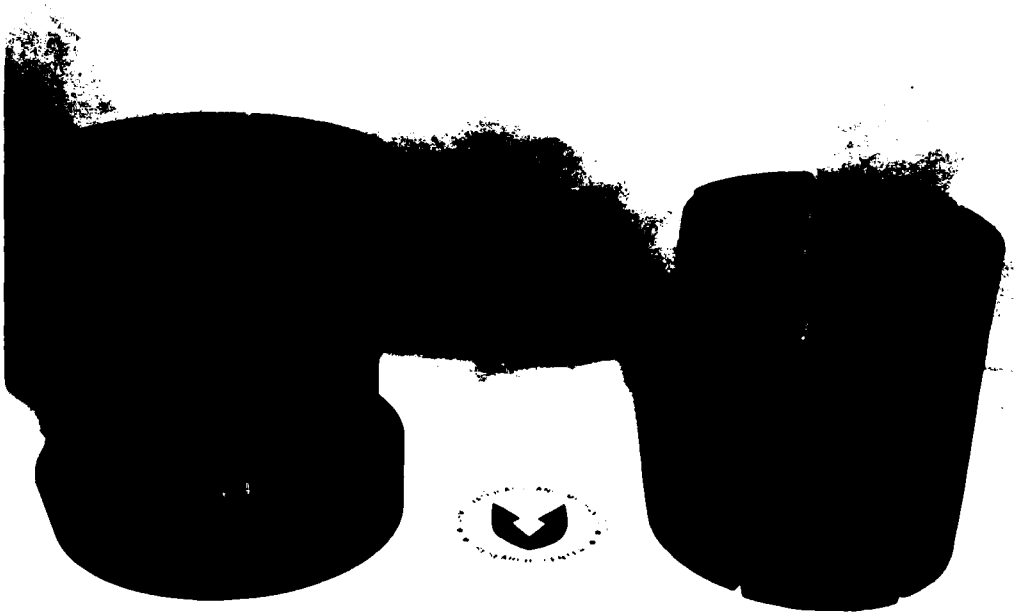

Figure 15. Photograph of graphite heating elements. Conventional ribbon element on the right side of the photograph. Note the thermal pitting and hot and cold spots alternation on the ribbon element. "Bird Cage" element on the left side of the photograph.

element at high temperatures requiring a high electric current, the power feeds have to be rigorously cooled by water. Consequently, they act as powerful heat sinks, thereby causing a decrease of the vertical thermal gradient. To remedy this problem, an element was inverted so that the power feeds were brought to the lower element ring. In this design, a sufficient upward gradient of 1.0°/mm over the 120-mm element heights was achieved. This element was adequate to enable growth of Nd:YAG single crystals 75 mm in diameter and 100 mm high. Since the gradient thus achieved proved to be still insufficient for growth of YAG crystals with a 100-mm diameter, a new type of "bird cage" element was designed and built. Because this element design has been submitted for patent proceedings and the patent is pending, no details can be given at the present time. This is the reason why the term "an upward thermal gradient" describing the thermal field imposed on the crucible containing both the growing crystal and the unused melt was previously introduced without any further comments.

CONCLUSIONS

Factors having a negative influence on the growth of large diameter single crystals were discussed in detail. Analysis of these factors revealed that the degree of their adverse action on crystal growth can be evaluated, and therefore their influence minimized, by imposing upon them a set of suitable ballancing conditions. Recognition of this principle led to a design of a new crystal growth technique (VSCOM) which allows growth of single crystals of certain compositions up to 250 mm in diameter, free of cracks, and second phase segregation.

DISTRIBUTION LIST

No. of Copies	To
	Office of the Under Secretary of Defense for Research and Engineering, The Pentagon, Washington, DC 20301
1	ATTN: Mr. J. Persh
1	Dr. G. Gamota
2	Commander, Defense Technical Information Center, Cameron Station, Building 5, 5010 Duke Street, Alexandria, VA 22314
1	National Technical Information Service, 5285 Port Royal Road, Springfield, VA 22161
	Director, Defense Advanced Research Projects Agency, 1400 Wilson Boulevard, Arlington, VA 22209
1	ATTN: LTC Loren Jacobson
1	Dr. Van Reuth
	Battelle Columbus Laboratories, Metals and Ceramics Information Center, 505 King Avenue, Columbus, OH 43201
1	ATTN: Mr. Winston Duckworth
1	Dr. D. Niesz
1	Dr. R. Wills
	CERES Corporation, 411 Waverly Oaks Park, Waltham, MA 02154
1	ATTN: Mr. J. Wencus
1	Mr. W. Menashi
	Commander, Army Research Office, P.O. Box 12211, Research Triangle Park, NC 27709
1	ATTN: Information Processing Office
1	Dr. G. Mayer
1	Dr. J. Hurt
	Commander, U.S. Army Materiel Command (AMC), 5001 Eisenhower Avenue, Alexandria, VA 22333
1	ATTN: AMCDM-ST, Dr. R. Haley
1	AMCLD, Dr. L. Hagen
1	AMCMT, Mr. F. J. Michel
	Commander, U.S. Army Electronics Research and Development Command, Fort Monmouth, NJ 07703
1	ATTN: AMDSD-L
1	T. Aucoin
	Commander, U.S. Army Materiel Systems Analysis Activity, Aberdeen Proving Ground, MD 21005
1	ATTN: AMXSY-MP, H. Cohen
	Commander, U.S. Army Night Vision Electro-Optics Laboratory, Fort Belvoir, VA 22060
1	ATTN: Director, Dr. L. Cameron
1	DELNV-L-D, Dr. R. Buser
1	Mr. Jeffrey L. Paul
	Commander, Harry Diamond Laboratories, 2800 Powder Mill Road, Adelphi, MD 20783
1	ATTN: Mr. A. Benderly
1	Technical Information Office
1	DELHD-RAE
	Commander, U.S. Army Missile Command, Redstone Arsenal, AL 35898
1	ATTN: Mr. P. Ormsby
1	Technical Library
1	AMSMI-TB, Redstone Scientific Information Center
1	AMSMI-EAT, Mr. Ray Farrison
1	AMSMI-EAT, Mr. Bobby Park
	Commander, U.S. Army Aviation Systems Command, 4300 Goodfellow Boulevard, St. Louis, MO 63120
1	ATTN: AMDAV-EGX
1	AMDAV-QE
1	Technical Library
	Commander, U.S. Army Natick Research and Development Center, Natick, MA 01760
1	ATTN: Technical Library
	Commander, U.S. Army Tank-Automotive Command, Warren, MI 48090
1	ATTN: Dr. W. Bryzik
1	Mr. Hamperian
1	D. Rose
1	AMSTA-ZSK
1	AMSTA-UL, Technical Library
1	AMSTA-R

No. of Copies	To
	Commander, U.S. Army Satellite Communications Agency, Fort Monmouth, NJ 07703
1	ATTN: Technical Document Center
	Commander, U.S. Army Armament, Munitions and Chemical Command, Dover, NJ 07801
1	ATTN: Mr. J. Lannon
1	Mr. Harry E. Pebly, Jr., PLASTEC, Director
1	Technical Library
	Commander, U.S. Army Armament, Munitions and Chemical Command, Rock Island, IL 61299
1	ATTN: Technical Library
	Commander, Aberdeen Proving Ground, MD 21005
1	ATTN: AMDAR-CLB-PS, Mr. J. Vervier
	Commander, U.S. Army Mobility Equipment Research and Development Command, Fort Belvoir, VA 22060
1	ATTN: AMDME-EM, Mr. W. McGovern
1	AMDME-V, Mr. E. York
1	AMDME-X, Mr. H. J. Peters
	Director, U.S. Army Ballistic Research Laboratory, Aberdeen Proving Ground, MD 21005
1	ATTN: AMDAR-TSB-S (STINFO)
	Commander, Rock Island Arsenal, Rock Island, IL 61299
1	ATTN: SARRI-EN
	Commander, U.S. Army Test and Evaluation Command, Aberdeen Proving Ground, MD 21005
1	ATTN: AMSTE-ME
	Commander, U.S. Army Foreign Science and Technology Center, 220 7th Street, N.E., Charlottesville, VA 22901
1	ATTN: Military Tech, Mr. W. Marley
	Director, Benet Weapons Laboratory, LCWSL, USA AMCCOM, Watervliet, NY 12189
1	ATTN: AMSMC-LCB-TL
	Commander, Watervliet Arsenal, Watervliet, NY 12189
1	ATTN: Dr. T. Davidson
1	ATTN: Dr. J. Ahmad
	Director, Eustis Directorate, U.S. Army Mobility Research and Development Laboratory, Fort Eustis, VA 23604
1	ATTN: Mr. J. Robinson, SAVDL-E-MOS (AVSCOM)
1	Mr. C. Walker
	Commander, U.S. Army Engineer Waterways Experiment Station, Vicksburg, MS 39180
1	ATTN: Research Center Library
	U.S. Army Munitions Production Base Modernization Agency, Dover, NJ 07801
1	ATTN: SARPM-PBM-P
	Technical Director, Human Engineering Laboratories, Aberdeen Proving Ground, MD 21005
1	ATTN: Technical Reports Office
	Chief of Naval Research, Arlington, VA 22217
1	ATTN: Code 471
1	Dr. R. Pohanka
	Naval Research Laboratory, Washington, DC 20375
1	ATTN: Dr. P. Klein
1	Mr. R. Rice
1	Dr. L. Esterowitz
	Headquarters, Naval Air Systems Command, Washington, DC 20360
1	ATTN: Code 5203
1	Code MAT-042M
1	Mr. C. F. Bersch
1	Mr. I. Machlin
	Headquarters, Naval Sea Systems Command, 1941 Jefferson Davis Highway, Arlington, VA 22376
1	ATTN: Code 035
	Headquarters, Naval Electronics Systems Command, Washington, DC 20360
1	ATTN: Code 504

No. of Copies	To
	Commander, Naval Ordnance Station, Louisville, KY 40214
1	ATTN: Code 85
	Commander, Naval Material Industrial Resources Office, Building 537-2, Philadelphia Naval Base, Philadelphia, PA 19112
1	ATTN: Technical Director
	Commander, Naval Weapons Center, China Lake, CA 93555
1	ATTN: Mr. F. Markarian
1	D. Dobberpuhl
1	Mr. M. Ritchie
	Commander, U.S. Air Force of Scientific Research, Building 410, Bolling Air Force Base, Washington, DC 20332
1	ATTN: MAJ W. Simmons
	Commander, U.S. Air Force Wright Aeronautical Laboratories, Wright-Patterson Air Force Base, OH 45433
1	ATTN: AFWAL/MLLM, Dr. N. Tallan
1	AFWAL/MLLM, Dr. H. Graham
1	AFWAL/MLLM, Dr. R. Ruh
1	AFWAL/MLLM, Mr. K. S. Mazdiyasni
1	Aero Propulsion Labs, Mr. R. Marsh
	Commander, Air Force Weapons Laboratory, Kirtland Air Force Base, Albuquerque, NM 87115
1	ATTN: Dr. Arthur Guenther
	Commander, Air Force Armament Center, Eglin Air Force Base, FL 32542
1	ATTN: Technical Library
	National Aeronautics and Space Administration, Washington, DC 20546
1	ATTN: Mr. G. C. Deutsch - Code RW
1	Mr. J. Gangler
1	AFSS-AD, Office of Scientific and Technical Information
	National Aeronautics and Space Administration, Langley Research Center, Center, Hampton, VA 23665
1	ATTN: Mr. J. Buckley, Mail Stop 387
	Commander, White Sands Missile Range, Electronic Warfare Laboratory, OMEW, ERADCOM, White Sands, NM 88002
1	ATTN: Mr. Thomas Reader, AMDEL-WLM-ME
	Department of Energy, Division of Transportation, 20 Massachusetts Avenue, N.W., Washington, DC 20545
1	ATTN: Mr. George Thur (TEC)
1	Mr. Robert Schulz (TEC)
1	Mr. John Neal (CLNRT)
1	Mr. Steve Wander (Fossil Fuels)
	National Bureau of Standards, Washington, DC 20234
1	ATTN: Dr. S. Wiederhorn
1	Dr. J. B. Wachtman
	National Research Council, National Materials Advisory Board, 2101 Constitution Avenue, Washington, DC 20418
1	ATTN: Dr. W. Prindle
1	D. Groves
1	R. M. Spriggs
	National Science Foundation, Washington, DC 20550
1	ATTN: B. A. Wilcox
	Adolf Meller Company, P. O. Box 6001, Providence, RI 02904
1	ATTN. Mr. Max E. Meller
	AVCO Corporation, Applied Technology Division, Lowell Industrial Park, Lowell, MA 01887
1	ATTN: Dr. T. Vasilos
	California Institute of Technology JPL 157-361, Pasadena, CA 91103
1	ATTN: Dr. P. J. Shlichta, Director of Material Science
	Case Western Reserve University, Department of Metallurgy, Cleveland, OH 44106
1	ATTN: Prof. A. H. Heuer
	Crystal Systems, Inc., P.O. Box 1057, Salem, MA 01970
1	ATTN: Mr. F. Schmid
	European Research Office, 223 Old Maryleborne Road, London, NW1 - 5the, England
1	ATTN: Dr. F. Rothwarf
1	LT COL James Kennedy

No. of Copies	To
	General Electric Company, Research and Development Center, Box 8, Schenectady, NY 12345
1	ATTN: Dr. R. J. Charles
1	Dr. C. D. Greskovich
	Georgia Institute of Technology, EES, Atlanta, GA 30332
1	ATTN: Mr. J. D. Walton
	GTE Laboratories, Waltham Research Center, 40 Sylvan Road, Waltham, MA 02154
1	ATTN: Dr. C. Quackenbush
1	Dr. W. H. Rhodes
	IIT Research Institute, 10 West 35th Street, Chicago, IL 60616
1	ATTN: Mr. S. Bortz, Director, Ceramics Research
	Electro-Optical and Data Systems Group, Hughes Aircraft Company, Culver City, CA 90230
1	ATTN: Dr. W. K. Ng
	Hughes Research Laboratories, A Division of Hughes Aircraft Company, 3011 Malibu Canyon Road, Malibu, CA 90265
1	ATTN: Dr. R. C. Pastor
1	Dr. Larry G. Shazer
	Lambda/Airtron Division, Litton Industries, 200 E. Hanover Avenue, Morris Plains, NJ 07950
1	ATTN: Dr. Roger Belt
1	Dr. Robert Uhrin
	Martin Marietta Laboratories, 1450 South Rolling Road, Baltimore, MD 21227
1	ATTN: Dr. J. Venables
	Massachusetts Institute of Technology, Department of Metallurgy and Materials Science, Cambridge, MA 02139
1	ATTN: Prof. R. L. Coble
1	Prof. H. K. Bowen
1	Prof. W. D. Kingery
1	Prof. A. Linz
	McDonnel Douglas Astronautics Company, Box 516, Saint Louis, MI 63166
1	ATTN: Dr. R. R. Rice
1	Dr. S. Thaler
	Midwest Research Institute, 425 Volker Boulevard, Kansas City, MO 64110
1	ATTN: Dr. K. P. Ananth
	Monsanto Electronic Products Division, P.O. Box 8, St. Peters, MI 63376
1	ATTN: Dr. Milan Kozak
	Norton Company, Worcester, MA 01606
1	ATTN: Dr. N. Ault
1	Dr. M. L. Torti
	Pennsylvania State University, Materials Research Laboratory, Materials Science Department, University Park, PA 16802
1	ATTN: Prof. R. Roy
1	Prof. R. E. Newnham
1	Prof. R. E. Tressler
1	Prof. R. Bradt
1	Prof. V. S. Stubican
	PSC, Box 1044, APO San Francisco 96328
1	ATTN: MAJ A. Anthony Borges
	RIAS, Division of the Martin Company, Baltimore, MD 21203
1	ATTN: Dr. A. R. C. Westwood
	Rockwell International Science Center, 1049 Camino Dos Rios, Thousand Oaks, CA 91360
1	ATTN: Dr. Ratnakar R. Neurgaonkar
	Sanders Associates, 95 Canal Street, Nashua, NH 03061
1	ATTN: MER, Mr. E. Chicklis
1	MER, Mr. T. Pollack
	Stanford Research International, 333 Ravenswood Avenue, Menlo Park, CA 94025
1	ATTN: Dr. P. Jorgensen
	State University of New York at Stony Brook, Department of Materials Science, Long Island, NY 11790
1	ATTN: Prof. Franklin F. Y. Wang

No. of Copies	To
	Sylvania Systems Group, Western Division, GTE Products Corp., P.O. Box 188, Mountain View, CA 94042
1	ATTN: Mr. Steve Guch
	United Technologies Research Center, East Hartford, CT 06108
1	ATTN: Dr. J. Brennan
1	Dr. F. Galasso
	U.S. Electronics Research and Development Command, 2800 Powder Mill Road, Adelphi, MD 20783
1	ATTN: AMDHD-TS, Dr. Robert Oswald
	University of California, Lawrence Livermore Laboratory, P. O. Box 808, Livermore, CA 94550
1	ATTN: Dr. M. J. Weber
1	Dr. C. F. Cline
	University of Florida, Department of Materials Science and Engineering, Gainesville, FL 32601
1	ATTN: Dr. L. Hench
	University of Washington, Ceramic Engineering Division, FB-10, Seattle, WA 98195
1	ATTN: Prof. James I. Mueller
	Varian Solid State West, 611 Hansen Way, Palo Alto, CA 94303
1	ATTN: Dr. Miro Vichr
	Westinghouse Electric Corporation, Research Laboratories, Pittsburgh, PA 15235
1	ATTN: Dr. R. J. Bratton
1	Dr. B. Rossing

No. of Copies	To
	Lincoln Laboratories, Massachusetts Institute of Technology, 24 Wood Street, Lexington, MA 02172
1	ATTN: Dr. Peter Moulton
	Naval Ocean Systems Center, 271 Catalina Blvd., San Diego, CA 92152
1	ATTN: Dr. Erhard Schimitscher - Code 84
1	Dr. Harry Rieger
	Phillips Laboratories, 345 Scarborouga Road, Briarcliff Manor, NY 10510
1	ATTN: Dr. Gabe Loiacono
1	Dr. Waltr Zwicker
	Union Carbide Corporation, 750 South 32nd Street, Washougal, WA 98671
1	ATTN: Dr. Jiin H. W. Liaw
1	Dr. Milan R. Kokta
	University of Oklahoma, Department of Physics Stillwater, OK 74074
1	ATTN: Dr. Richard C. Powell
	Director, Army Materials and Mechanics Research Center, Watertown, MA 02172-0001
2	ATTN: AMXMR-PL
1	Author

END

FILMED

1-85

DTIC